Complimentary and personal copy for

Joseph H. Lorent, Catherine Léonard, Marthe Abouzi, Farida Akabi, Joëlle Quetin-Leclercq, Marie-Paule Mingeot-Leclercq

www.thieme.com

α-Hederin Induces Apoptosis, Membrane Permeabilization and Morphologic Changes in Two Cancer Cell Lines Through a Cholesterol-Dependent Mechanism

DOI 10.1055/s-0042-114780
Planta Med

This electronic reprint is provided for non-commercial and personal use only: this reprint may be forwarded to individual colleagues or may be used on the author's homepage. This reprint is not provided for distribution in repositories, including social and scientific networks and platforms.

Publishing House and Copyright:
© 2016 by
Georg Thieme Verlag KG
Rüdigerstraße 14
70469 Stuttgart
ISSN 0032-0943

Any further use
only by permission
of the Publishing House

α-Hederin Induces Apoptosis, Membrane Permeabilization and Morphologic Changes in Two Cancer Cell Lines Through a Cholesterol-Dependent Mechanism

Authors

Joseph H. Lorent[1,2], Catherine Léonard[1], Marthe Abouzi[1], Farida Akabi[1], Joëlle Quetin-Leclercq[2], Marie-Paule Mingeot-Leclercq[1]

Affiliations

[1] Université catholique de Louvain, Louvain Drug Research Institute, Cellular and Molecular Pharmacology, Bruxelles, Belgium
[2] Université catholique de Louvain, Louvain Drug Research Institute, Pharmacognosy, Bruxelles, Belgium

Key words
- saponin
- triterpenic acid
- apoptosis
- membrane permeabilization
- cholesterol

received March 18, 2016
revised July 21, 2016
accepted August 4, 2016

Bibliography
DOI http://dx.doi.org/10.1055/s-0042-114780
Published online
Planta Med © Georg Thieme Verlag KG Stuttgart · New York · ISSN 0032-0943

Correspondence
Prof. Dr. Marie-Paule Mingeot-Leclercq
UCL B1.73.05
Université catholique de Louvain – Louvain Drug Research Institute
Cellular and Molecular Pharmacology – Pharmacognosy
Avenue E. Mounier 73
B-1200 Bruxelles
Belgium
Phone: + 32 27 64 73 74
marie-paule.mingeot@uclouvain.be

Abstract

In perspective of reducing the mortality of cancer, there is a high interest in compounds which act on multiple cellular targets and therefore prevent the appearance of cancer resistances. Saponins and α-hederin, an oleanane-type saponin, induce cancer cell death through different pathways, including apoptosis and membrane permeabilization. Unfortunately, the mechanism by which cell death is induced is unknown. We hypothesized that the activity of α-hederin mainly depends on its interaction with membrane cholesterol and therefore investigated the cholesterol and saponin-structure dependency of apoptosis and membrane permeabilization in two malignant monocytic cell lines. Apoptotic cell death and membrane permeabilization were significantly reduced in cholesterol-depleted cells. Permeabilization further depended upon the osidic side chain of α-hederin and led to extracellular calcium influx and nuclear fragmentation, with only the latter being susceptible to caspase inhibitors. Membrane order, measured by laurdan generalized polarization imaging, was neither reduced by α-hederin nor its aglycone hederagenin suggesting that their activity was not related to membrane cholesterol extraction. However, a radical change in morphology, including the disappearance of pseudopodes was observed upon incubation with α-hederin. Our results suggest that the different activities of α-hederin mainly depend on its interaction with membrane cholesterol and consequent pore formation.

Abbreviations

AO/EB:	acridine orange/ethidium bromide
BCA:	bicinchonic acid
BSA:	bovine serum albumin
DAPI:	4′,6-diamidino-2-phenylindole
EGTA:	ethylene glycol-bis(β-aminoethyl ether)-N,N,N′,N′-tetraacetic acid
FCS:	fetal calf serum
MβCD:	methyl-β-cyclodextrin
SDS:	sodium dodecyl sulfate

Supporting information available online at http://www.thieme-connect.de/products

Introduction

Cancer is becoming an increasing problem of public health especially in developed countries. The appearance of cancer resistance towards conventional chemotherapy diminishes the chances of successful treatment and is therefore a major challenge in cancer research [1]. A way to prevent chemotherapeutic resistance in cancer cells is to act on multiple targets. Saponins, natural amphiphilic compounds have shown the potential to induce cancer cell death by multiple pathways and to increase the activity towards common chemotherapeutic agents or radiotherapy [2–5]. α-Hederin (kalopanaxsaponin A, **Fig. 1S**, Supporting Information), an oleanane type saponin extracted from *Hedera helix*, showed a promising activity *in vivo* against colon and lung cancer [5]. It has been shown that α-hederin possesses a selective cytotoxic activity towards cancer cells most probably by activating on apoptotic pathways via cytosolic increase of reactive oxygen species and Ca^{2+} [6, 7]. We recently showed that α-hederin and its aglycone hederagenin (**Fig. 1S**, Supporting Information) were able to induce pore formation in liposomal systems in a cholesterol dependent manner [8]. Because cholesterol plays a critical role for both the activity on cancer cells and hemolysis by saponins [9], the characterization of the interaction between α-hederin and cholesterol in cell

		Non-depleted	Depleted
U937	Cholesterol/proteins	13.13 ± 1.30 µg/mg	4.49*** ± 0.24 µg/mg
	Cholesterol/phospholipids	150.90 ± 14.98 µg/µM	40.26*** ± 2.16 µg/µM
THP-1	Cholesterol/proteins	11.29 ± 0.39 µg/mg	6.54*** ± 0.72 µg/mg
	Cholesterol/phospholipids	129.93 ± 4.17 µg/µM	60.07*** ± 6.67 µg/µM

Three independent experiments have been performed, Statistical analysis: One-way ANOVA. ***p < 0.001

Table 1 Ratios of cholesterol/proteins and cholesterol/phospholipids in non-depleted and cholesterol depleted U937 and THP-1 cells.

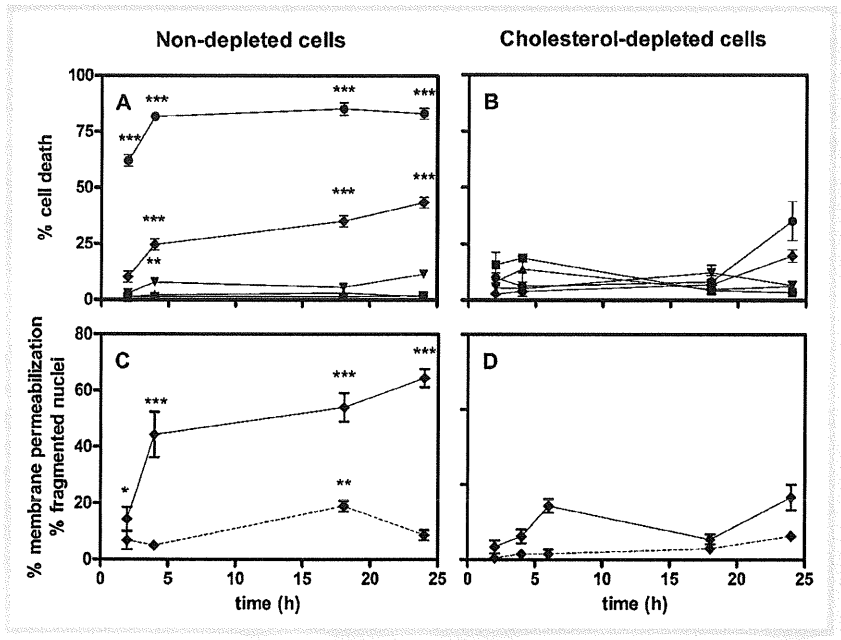

Fig. 1 Cytotoxicity induced by α-hederin in non-depleted (**A, C**) and cholesterol-depleted U937 cells (**B, D**). Panels **A** and **B** show trypan blue assay of cells incubated with increasing concentrations of α-hederin: Control (■), 10 µM (▲), 15 µM (▼), 20 µM (♦) and 25 µM (●). Panels **C** and **D** display acridine orange/ethidium bromide assay of cells incubated with 20 µM of α-hederin. Straight line: Cells with permeabilized plasma membrane, dashed line: cells with fragmented nuclei. Three independent experiments were performed. Statistical analysis: Two-way ANOVA between non-depleted and cholesterol depleted conditions. *P < 0.5; **p < 0.1; ***p < 0.01.

membranes is a key for the understanding of the mechanisms involved in saponin induced cell death. The interaction of α-hederin with membraneous cholesterol could also have repercussions on the chemotherapeutic resistance of cancer cells since its regulatory function on the membrane order has been put into relationship with the activity of drug expelling channels [10]. However, several saponins changed the lipid order in cell membranes but no consistency was observed among those compounds regarding an increase or decrease of membrane fluidity or whether this change was cholesterol related or not [11, 12]. Interestingly, ginsenoside Rg3 induced changes in the membrane order responsible for a reduction of chemotherapeutic resistance in multidrug resistant cancer cells [13].

Hence, the activity of saponins and α-hederin might depend on their interaction with cholesterol in the plasma membrane. We therefore decided to analyze the importance of cholesterol in α-hederin induced cell death in cancer cells and the effects of the saponin on plasma membrane integrity and order. As a model, we used two monocytic cell lines depleted or not in cholesterol: U937, a cholesterol auxotroph cell line [14] and THP-1 cells, able to synthesize their own cholesterol [15]. In addition, we established the importance of the sugar moiety for those effects, by comparing the effect of α-hederin with that obtained with its aglycone, hederagenin.

Results

MβCD was very efficient in reducing the cholesterol/protein and cholesterol/phospholipid ratio in U937 and THP-1 cells (**Table 1**). The phospholipid amount was not influenced by MβCD (data not shown), indicating a selective depletion of cholesterol. The measured cholesterol concentrations of non-depleted cells corresponded almost to values reported in literature [16, 17].

Cell death was rapidly observed in α-hederin treated U937 cells by trypan blue assay. It increased upon α-hederin concentration. At the highest concentration investigated (25 µM; **Fig. 1A**), α-hederin induced 62 ± 5.2% of cell death after 2 h of incubation. Depletion of cholesterol by MβCD effectively reduced α-hederin induced cell death in U937 cells upon 18 h of incubation (**Fig. 1B**). These observations agree with those previously obtained on THP-1 cells [8]. SDS, conversely to α-hederin induced cell death preferentially in cholesterol-depleted cells (**Fig. 2S**, Supporting Information). This confirms that only the saponin toxicity was inhibited by cholesterol depletion.

Monitoring the cholesterol-dependency of α-hederin induced cell death by acridine orange/ethidium bromide staining (**Fig. 1C, D**) allowed us to follow the permeabilization of the plasma membrane in parallel with changes of the nucleus' morphology. The fragmentation of the nucleus is usually regarded as a sign of apoptotic cell death but might also occur to a lesser extend in necrosis [18]. Membrane permeabilization and the subsequent influx of ethidium bromide were induced long before the appearance of nucleus fragmentation. More than 40% of the cells lost their membrane integrity after 4 h of incubation with 20 µM

Electronic reprint for personal use

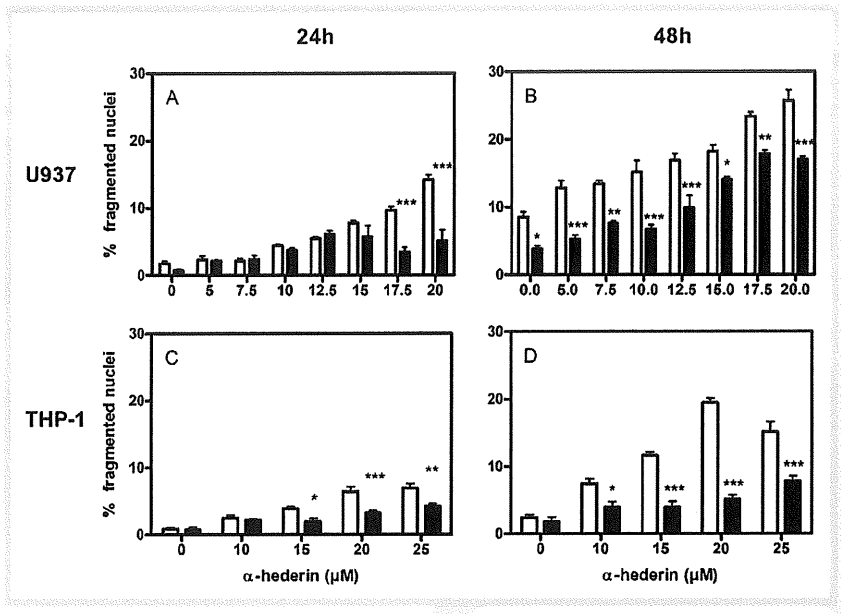

Fig. 2 Apoptosis induced by α-hederin in U937 (**A, B**) and THP-1 (**C, D**) cells, depleted or non- depleted in cholesterol. Fragmentation of nucleus of depleted (black bars) or non-depleted (white bars) cells incubated for 24 (**A, C**) and 48 h (**B, D**) with increasing concentrations of α-hederin. Statistical analysis: One-way ANOVA: depleted vs. non-depleted cells. *P < 0.05; **p < 0.01; ***p < 0.001.

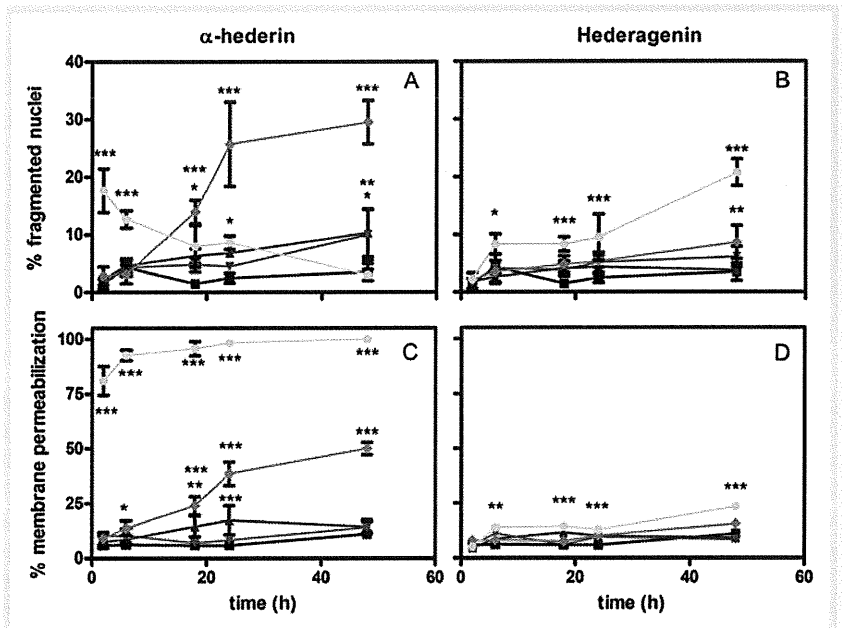

Fig. 3 Apoptosis (% fragmentated nuclei) and cell necrosis (% membrane permeabilization) induced by α-hederin and its aglycone, hederagenin. Panels **A, B, C, D**: U937 cells incubated for 2, 6, 18, 24 and 48 h with α-hederin (**A, C**) or hederagenin (**B, D**). Control (■, black), 10 μM (▲, very dark grey), 15 μM (▼, dark grey), 20 μM (♦, grey) and 40 μM (•, light grey). Statistical analysis: Two-way ANOVA: vs. control. *P < 0.05; **p < 0.01; ***p < 0.001.

of α-hederin in non-depleted cells. Nucleus fragmentation became significant after 18 h of incubation. Depletion of cholesterol reduced the fragmentation of the nucleus. Membrane defects were also reduced in depleted cells (**Fig. 1D**) which confirmed the results obtained with trypan blue assay (**Fig. 1A**).

Fragmentation of nuclei was further investigated in a concentration-dependent manner by DAPI assay for 24 and 48 h. Fragmentation increased upon α-hederin concentration in U937 (**Fig. 2A, B**) and THP-1 cells (**Fig. 2C, D**). In THP-1, as well as in U937 (not shown), a maximum of fragmentation could be observed at concentrations around 20 μM. In all conditions investigated, depletion of cholesterol reduced the fragmentation of the nuclei.

The osidic side chain of α-hederin has been shown to play an important role in the formation of pores in giant unilamellar vesicles (GUV) [19]. We therefore investigated the critical role of sugars in the membrane permeabilization and cell death (**Fig. 3**). Hederagenin has the same triterpenoid backbone as α-hederin but lacks the sugar moiety. We compared the effects of α-hederin (**Fig. 3A, C**) and hederagenin (**Fig. 3B, D**) on U937 cells using AO/EB assay.

Consistently with results shown for the trypan-blue assay (**Fig. 1A**), α-hederin induced a very rapid cytosolic ethidium bromide influx at higher concentrations (**Fig. 3C**). This effect was not observed with hederagenin even at very long incubation periods (**Fig. 3D**). Condensation and fragmentation of nuclei was induced very soon after addition of 40 μM of α-hederin but decreased for longer incubation periods. The cells presenting nuclear fragmentation at this concentration systematically presented ethidium bromide influx. The highest effect on fragmentation was observed with 20 μM of α-hederin for 24 and 48 h of incubation (**Fig. 3A**). Hederagenin only induced fragmentation after

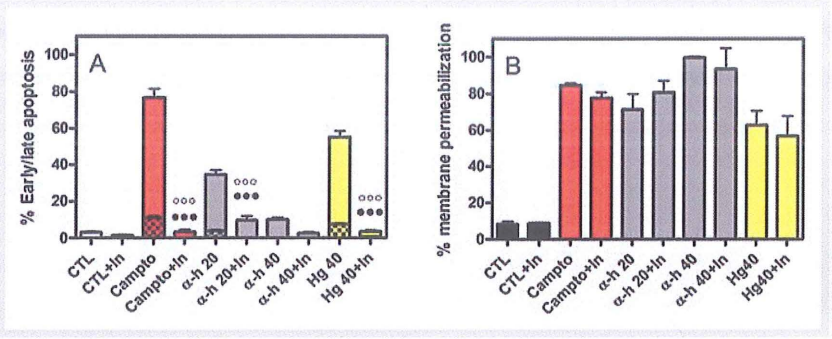

Fig. 4 Effect of caspase inhibitor on apoptosis and membrane permeabilization. Panels **A, B** U937 cells were incubated for 48 h with camptothecine (Campo, red), α-hederin (α-h, grey), hederagenin (Hg, yellow) with or without pan-caspase inhibitor Q-Vd-OPh (In). **A** Early (patterned bar)/late (not patterned bar) apoptosis and **B** membrane permeabilization. CTL is the control. Statistical analysis: One-way ANOVA; symbols: • = Early apoptosis ± inhibitor ○ = Late apoptosis ± inhibitor; three symbols: $p < 0.001$.

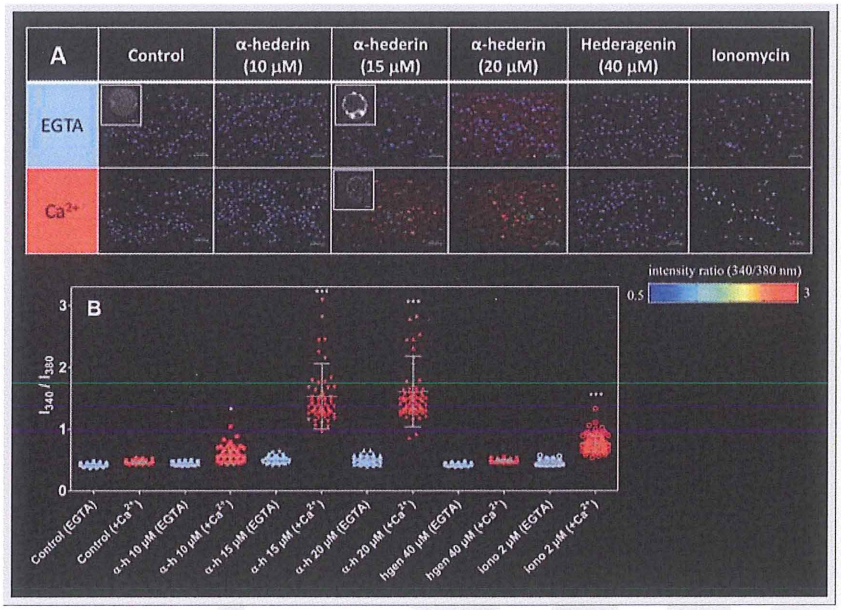

Fig. 5 Calcium influx: U937 cells have been labeled with Fura-2 AM and further incubated for 30 min at room temperature in KREBS media containing 250 µM EGTA or 1.5 mM $CaCl_2$ and α-hederin, hederagenin or ionomycin as positive control. In panel **A**, cells are pseudocolored upon the intensity ratio of Fura-$2_{bound\ to\ Ca^{2+}}$/Fura-$2_{unbound}$ (I_{340}/I_{380}). The colors range from 0.3 (deep blue) to 2.5 (red) and scale bars are equal to 50 µm. Inserts show a biphoton microscopy slide (scale bars are 5 µm) of a representative cell for the control and conditions where a significant change has been observed. Panel **B** represents the intensity ratio of at least 70 cells from two independent experiments for each condition. Blue symbols represent EGTA and red symbols the Ca^{2+}-containing condition. Statistical analysis: One way ANOVA has been performed separately for EGTA and Ca^{2+}-containing media. $^{*}P < 0.05$, $^{***}p < 0.001$ compared to the control.

48 h at 40 µM which is close to the solubility limit of the compound (**Fig. 3B**).

Moving on the mechanism involved in cell death and fragmentation of the nucleus by α-hederin and hederagenin, we investigated the role of caspases by preincubating cells with the pan-caspase inhibitor Q-VD-OPh (**Fig. 4A, B** and **Fig. 3S**, Supporting Information). After 48 h of incubation with α-hederin and hederagenin, Q-VD-OPh effectively inhibited fragmentation of the nucleus but did not significantly reduce the cytosolic ethidium bromide influx for both compounds. In addition, the proportion of early apoptosis compared to all cells with fragmented nuclei was very low also for shorter incubation periods (**Fig. 4A** and **Fig. 3S** (**C, D**), Supporting Information). Camptothecine induced nuclear fragmentation and cell death was efficiently reduced by Q-VD-OPh especially at shorter incubation times (**Fig. 3S**, Supporting Information) and agrees with data obtained on HL-60 cells [20]. At 4 h of incubation and 40 µM α-hederin, caspase inhibition by Q-VD-OPh did not reduce the membrane permeabilization, suggesting a caspase independent cell death at high saponin concentrations (**Fig. 3S** (**B**), Supporting Information).

Calcium influx in monocytes has been compared for α-hederin, hederagenin and ionomycin. α-Hederin induced calcium influx in a concentration- and time-dependent manner. After 30 min of incubation with α-hederin, no significant calcium influx was observed at 10 µM, but several cells showed a higher intensity ratio of FURA-2 (I_{340}/I_{380}) which reflects a higher intracytosolic Ca^{2+}-concentration compared to the control. This was only observed in media containing extracellular Ca^{2+} (**Fig. 5A, B**). The cytosolic Ca^{2+}-influx induced a significant change of the intensity ratio at 15 and 20 µM of α-hederin in Ca^{2+}-containing media. Extracellular EGTA reduced effectively the intensity ratio in α-hederin incubated cells suggesting an extracellular influx. The overall intensity of the FURA-2 signal was reduced at 15 and 20 µM, reflecting a leak of the fluorescent marker out of the cells. Interestingly, several cells treated with α-hederin concentrated FURA-2 into spots whereas a homogenous distribution of the marker was kept in other conditions (**Fig. 5A**). Biphoton microscopy (insets) revealed that this effect occurred even in the presence of EGTA suggesting it did not exclusively depend on extracellular Ca^{2+}. Hederagenin (40 µM) did not induce an increase of the intensity ratio, indicating a lack of cytosolic Ca^{+2}-increase.

At 40 µM, α-hederin induced rapid (less than 5 min) intracytosolic calcium influx (**Fig. 4S**, Supporting Information). The intensity ratio increased from 0.5 for control cells to 1.5 after 5 min treatment. Conversely to ionomycin, this increase did not depend on extracellular calcium (1.5 mM) which suggests that, at this concentration, α-hederin induces not only the influx of extracellular calcium but also the release of intracellular calcium stores. Additionally, the signal intensity of FURA-2 decreased, reflecting a leak out of FURA-2 from the cell. After 30 min of incubation and 40 µM of α-hederin, all the FURA-2 had been leaked from cells and they were no longer fluorescent (data not shown).

Electronic reprint for personal use

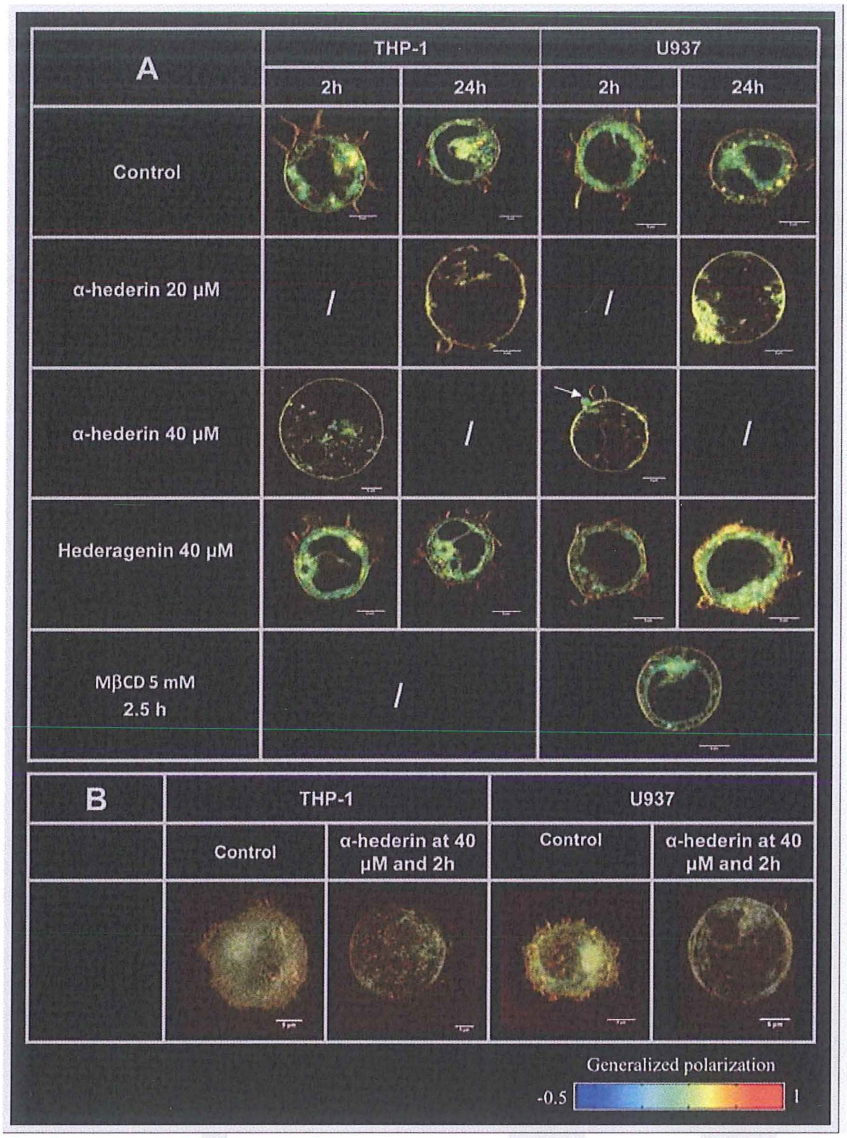

Fig. 6 GP-images of THP-1 and U937 cells, incubated with α-hederin (20, 40 μM) or hederagenin (40 μM) for 2 and 24 h. **A** Confocal sections in the middle plane of the cell. As a control, cells have been incubated with MβCD (5 mM) for 2.5 h. **B** 3D-reconstructions of GP-confocal sections for negative controls and at 2 h and 40 μM of α-hederin. GP-images are pseudocolored ranging from −0.5 (blue) to 1 (red). Scale bar = 5 μM.

At a glance, intracytosolic calcium is significantly increased by α-hederin and at high concentrations, FURA-2 leak out is observed suggesting the formation of larger non Ca^{2+}-selective pores even at short incubation times. Hederagenin itself was not able to increase Ca^{2+}-influx at 40 μM and 30 min of incubation.

We further investigated the effect of α-hederin and hederagenin on morphology as well as on membrane order in macrophages. We used laurdan biphoton microscopy to determine generalized polarization (GP) of cell membranes. Laurdan-GP is an indicator of membrane order at the water-membrane interface. Higher GP-values reflect a lower polarity of the microenvironment of the fluorescent probe and can generally be associated with higher lipid packing in the membrane.

The GP of plasma membranes in U937 and THP-1 cells was always higher than the GP of intracellular membranes. This particularity has been shown in other cell lines and might be attributed to the higher content of cholesterol and saturated lipids of the plasma membrane, compared to intracellular organelles [21]. Hence, it permits to distinguish between the plasma membrane and intracellular membrane material (**Fig. 6**). GP values from the plasma membranes are represented as GP_{high} and all other GP values are represented as GP_{low} (**Fig. 5S**, Supporting Information).

Membrane morphology of U937 and THP-1 cells was radically changed upon incubation with α-hederin (**Fig. 6**). After 2 h of incubation with 40 μM, pseudopodes disappeared which gave the impression of a 'flat'-spherical plasma membrane (**Fig. 6A, B**). This effect was also observed at 24 h incubation with 20 μM of α-hederin (**Fig. 6A**). MβCD induced a similar effect which might indicate a cholesterol dependence of this effect. In addition, we observed the formation of plasma membrane blebs with 20 and 40 μM of α-hederin after 24 and 2 h of incubation, respectively. Those changes on the plasma membrane were accompanied by a release of intracellular membrane material to the extracellular media (see arrow) which made the cells resemble ghost cells. The shape of the nucleus was transformed from bilobar to spherical, which was occasionally accompanied by nuclear fragmentation.

In parallel, upon α-hederin incubation, we observed an overall increase of GP values in both cell types but this effect seemed to be more important for GP_{low} and GP_{mean} values (**Fig. 5S**, Supporting Information). This was most probably due to the fact that the intracellular membrane material was either disintegrated or re-

Electronic reprint for personal use

leased to the membrane exterior. The plasma membrane order (GP_{high}) in U937 cells remained unchanged. This was different to THP-1 cells, where plasma membrane order (GP_{high}) seemed to increase compared to the control. As a positive control for plasma membrane order reduction (GP_{high}), we used 5 mM of MβCD in RPMI media containing 1 mg/mL BSA and exempt of FCS. In those conditions, GP values (low, high and mean) were significantly reduced and generally attributed to the depletion of membrane cholesterol (**Fig. 5S**, Supporting Information) [22].
Hederagenin did neither have an effect on cell membrane morphology nor on membrane order for at least 24 h of incubation at its solubility limit of 40 µM.

Discussion

In the past, α-hederin has been shown to induce apoptotic features like DNA fragmentation and caspase dependent cell death. It has been assumed that the saponin would be able to induce apoptotic pathways via activation of specific Ca^{2+}-channels and depletion of antioxidant species in the cytoplasm [6,7]. In addition to this effect, direct pore formation was observed but a link between both activities was so far missing [23].
Through our results it emerges that the main component of α-hederin induced cell death can be attributed to its membrane permeabilizing activity, especially at high concentrations, which seems to be related to the presence of cholesterol in the membrane. Several results point into this direction: (i) treated cells with fragmented nuclei present mostly a compromised cell membrane and ethidium bromide influx. They might still be seen as "late apoptotic" cells but at 2 h of incubation with 40 µM, the percentage of ethidium bromide influx is already at 75%. (ii) Total cell death is not reduced by general caspase inhibitors at short incubation times, conversely to campthotecin (**Fig. 3S**, Supporting Information). (iii) Depletion of cholesterol confers resistance towards α-hederin induced cell death. Pore formation in liposomal membranes by α-hederin has been shown to be cholesterol dependent [8] and lysis of red blood cells by saponins was explained by a cholesterol dependent mechanism [24]. The depletion of cholesterol in the plasma membrane of cancer cells should hence refer resistance to pore formation. (iv) Cytosolic Ca^{2+}-influx is concentration- and time-dependent. At 15 and 20 µM, influx depends mainly on extracellular calcium. It has been shown previously that pores formed by α-hederin in GUV and LUV increased their size through a concentration and time-dependent way [8,19]. This is also supported by the fact that FURA-2, a larger molecule than Ca^{2+}, only escapes from the cells at high saponin concentrations (**Fig. 5S** (**A**), Supporting Information). Calcium influx might also be the trigger for several apoptotic hallmarks as it was proposed previously [6]. Apoptosis induction would in this case depend, at least in part, on pore formation by α-hederin. At 40 µM, α-hederin induced cytosolic Ca^{2+}-influx even when no Ca^{2+} was present in the extracellular media. This means that the saponin is also able to perforate membranes of intracellular calcium stores at high concentration. (v) Cells loose their intracellular organelles upon incubation with high concentrations of α-hederin. A part of the intracellular membrane material was released to the cell exterior which suggests relatively large pores (**Fig. 6**). (vi) The direct morphological changes on the plasma membrane as well as the flattening or the formation of blebs might indicate a direct effect on the membrane. Inhibition of pseudopodia formation by α-hederin and MβCD accounts for a cholesterol-dependency of this effect. It has been shown on macrophages, that the formation of pseudopodes is a cholesterol dependent mechanism [25,26]. Formation of blebs is an apoptotic hallmark [27] but could be related to the curvature stress which is generated by α-hederin [8].
Despite all the data, it is not exactly clear which type of pore, membrane hole or instability is induced by α-hederin. Our recent studies on membrane models showed that α-hederin can induce the formation of large toroidal pores at high concentration, but it was also shown that at lower concentrations the saponin induced rather the formation of lipid aggregates in the membrane, which were composed of phospholipids and sterols. The formation of those aggregates might deplete the membrane of its lipid material and create transient or permanent membrane instabilities and holes [8,19]. The increase of laurdan generalized polarization in the plasma membrane might indicate the formation of similar aggregates (**Fig. 5S**, Supporting Information) but to resolve this issue, it would require further investigation. Both mechanisms coexist most probably and might depend on the critical micellar concentration of the saponin [19]. Similarly, amphotericin, an antifungal compound, induced the formation of pores and a "sponge"-like phase, which was able to sequester membrane ergosterol and thereby decrease membrane stability [28]. However, since the effects of α-hederin were not accompanied by a decrease of plasma membrane order, as it has been observed with MβCD, an extraction of cholesterol from the membrane into the surrounding media is less probable (**Fig. 5S**, Supporting Information).
We further wanted to point out the importance of the sugar chain in cell death induction. Regarding the structure of the saponin, we showed that the presence of the sugar chain was critical for rapid cell death induction but didn't seem necessary for cell death induction at longer incubation periods. Without the sugar chain (hederagenin), there was neither a rapid cell death nor membrane permeabilization observed at concentrations up to 40 µM. This can probably be put into relationship with the results obtained in GUV at high concentration, where an immediate permeation to dextran at 4 kDa was observed with α-hederin whereas the effect with hederagenin became only evident at 48 h of incubation [8]. Induction of cell death required longer incubation periods and higher concentrations with hederagenin compared to α-hederin.
Despite the effect on membrane permeabilization, the extrinsic apoptotic pathway could also play a role, especially at lower concentrations. For avicin D, another saponin, depletion of membrane cholesterol by MβCD inhibited activation of death receptors in cancer cells [29]. Activation of death receptors via coalescence or disruption of lipid rafts has also been shown for some other saponins and cholesterol binding toxins [30,31]. The induction of phase separation in GUVs mimicking nanoscopic raft domains by α-hederin supports this hypothesis [19].
Regarding the potential use of both drugs as anticancer agents, the present study shows that α-hederin induces cell death in cancer cells very efficiently. However, the question arises how the present mechanism could be in any way specific towards cancer cells. Some specificity might arise from an overproduction of cholesterol in several types of cancer cells as a higher membrane cholesterol content would mean a more efficient membrane destabilization or apoptosis induction by the saponin [32,33]. Since α-hederin given intraperitoneal had an effective anticancer activity in mice against two very resilient cancer types, its limitation

Electronic reprint for personal use

due to hemolytic effects [34] might only apply when administered directly into the blood stream.
At a glance, α-hederin induces cell death via cholesterol dependent pore formation followed by cytosolic Ca^{2+}-influx mostly from extracellular media. The pore formation involves the release of intracellular membrane material from the cell. The pore forming activity would not be due to a cholesterol extraction from the membrane but rather due to the formation of cholesterol/saponin aggregates in the membrane which do not involve a general change of membrane order. This effect might further lead to the inhibition of pseudopodia formation. We also show that the caspase-dependent fragmentation of the nucleus is most probably due to the increase of cytosolic Ca^{2+} after membrane permeabilization of cancer cells [35].

Material and Methods

Chemicals, biochemicals and cell lines

α-hederin and hederagenin (purity ≥ 98%) were purchased from Extrasynthèse. The compounds were dissolved in ethanol. After evaporation of the solvent, the residue was resolubilized in RPMI media containing 0,1% of DMSO in an ultrasonic bath for 5 min. Corresponding controls were used. Cells were purchased from ATCC. RPMI medium was ordered by Life technologies. BCA protein assay, FURA-2 AM, ionomycin (purity > 90%) and Amplex red cholesterol assay kit were purchased from ThermoFisher Scientific. MβCD, SDS, DAPI, acridine orange and ethidium bromide were ordered from Sigma-Aldrich. All other reagents were ordered from E. Merck AG.

Cell culture, cholesterol depletion and incubation with α-hederin and hederagenin

All our experiments were performed on cells which were freshly defrozen from a stock, that had been established directly after purchasing the cells from ATCC. Cell cultures were never kept longer than 3 weeks in culture. Cells were cultivated in RMPI medium containing 10% FCS in 95% air and 5% CO_2.
For cholesterol depletion, cells (10^6 cells/mL) were incubated for 2.5 h in RPMI medium containing 1 mg/mL BSA and 5 mM MβCD. Cell counting was performed in a Burker chamber. After incubation, cells were washed 3 times with RPMI medium without serum.
At this time, a part of the cells were quantified for their cholesterol, phospholipid and protein contents. For cholesterol and phospholipid quantification, cellular lipids were first extracted [36] and further quantified by Amplex red cholesterol assay and phosphorus assay [37]. Proteins were quantified by the BCA protein assay kit.
For further incubation with α-hederin, hederagenin or SDS, cholesterol-depleted cells were incubated in RPMI media containing 10% FCS.

Determination of cell death

Cell death was quantified by the trypan blue assay using a phase contrast microscope and results were expressed in % of total cells [38].

Determination of cell nucleus fragmentation and integrity of the plasma membrane

We used DAPI assay to determine nuclear fragmentation [39]. A total of 500 cells was counted.
To distinguish between living, death cells and early and late apoptosis, we used the AO/EB assay [40]. Both stains label the nucleus but only acridine orange can diffuse through an intact plasma membrane. After incubation, cells were harvested and washed in PBS medium. They were then put in contact with the AO/EB (100 µg/mL) solution and observed by fluorescence microscopy. Early apoptotic cells had a fragmented nucleus and presented no EB influx. All the cells showing EB influx were counted as cells with a defect membrane. Cells presenting both EB influx and nucleus fragmentation were considered as late apoptotic. A total of 200 cells were counted.

Determination of extracellular calcium influx by microspectrofluorimetry

U937 cells were loaded with FURA-2 AM for 1 h at 20 °C in RPMI medium containing 10% FCS. They were further washed with KREBS-HEPES media (+BSA 1 mg/mL) adjusted at pH = 7.4 and incubated in the same media containing 1.5 mM $CaCl_2$ or 250 µM EGTA. α-hederin and hederagenin were resuspended in the corresponding buffer solution with 0.1% DMSO. For microscopy, cells were transferred into non coated IBIDI slides and alternatively excited at 340 and 380 nm. Emission fluorescence was monitored at 510 nm using a Deltascan spectrofluorimeter (Photon Technology International) coupled to a Nikon Diaphot inverted microscope (Fluar 20×, objective; numerical aperture, 0.75). Fluorescence intensity was recorded over the surface of each single cell and intracytosolic $[Ca^{2+}]$ was evaluated from the ratio of the fluorescence emission intensities excited at both wavelengths. A minimum of 30 cells have been analyzed for each condition.

Biphoton microscopy of laurdan in monocytes

After incubation, cells were washed with RPMI media and labeled with laurdan at 2 µM and 37 °C for 30 min in RPMI media (+ 1 mg/mL BSA). They were further washed with PBS at pH = 7.4 and transferred in the same buffer to IBIDI slides. Excitation was done at 780 nm (0.5% intensity) and cells were observed using a C-Apochromat 63×/1.2 water immersion objective. Emission intensity was recorded upon two channels ($I_1 = I_{404-457}$ nm and $I_2 = I_{468-528}$ nm) on entire cells. Generalized polarization (GP) was calculated using the formula: $GP = (I_1 - G.I_2)/(I_1 + G.I_2)$. The G-factor (G) is instrument dependent and was determined through a calibration method previously described [41]. Generalized polarization (GP) images (HSV images) were created with a own Matlab routine based on principles previously established [41]. Briefly, all GP-values of an obtained GP-image were fitted to a double Gaussian function. The centre of both functions were represented by two GP values (GP_{high} and GP_{low}), reflecting approximately the GP-values of the plasma membrane and the intracellular membranes, respectively (see results). GP_{mean} represented the total average of all GP-values in a cell. A total of 15 entire cells was analyzed for each condition.

Supporting information

Structures of α-hederin and hederagenin as well as results and additional data are available as Supporting Information.

Acknowledgements

We thank the laboratory of cell biology for the disposition of their biphoton microscope (LSM 510 NLO, Zeiss) and especially Patrick Van Der Smissen for his skillful help. We also appreciated the

Document is copyright for personal use

work of Nicolas Tajeddine for the calcium release assays and Marie-Claire Cambier for her help on cell culture. We also thank the Université Catholique de Louvain for the "Bourse du patrimoine" grant which permit part of this work.

Conflict of Interest

The authors declare no conflict of interest.

References

1 *Holohan C, Van Schaeybroeck S, Longley DB, Johnston PG.* Cancer drug resistance: an evolving paradigm. Nat Rev Cancer 2013; 13: 714–726
2 *Lee SJ, Sung JH, Lee SJ, Moon CK, Lee BH.* Antitumor activity of a novel ginseng saponin metabolite in human pulmonary adenocarcinoma cells resistant to cisplatin. Cancer Lett 1999; 144: 39–43
3 *Jiang H, Zhao P, Feng J, Su D, Ma S.* Effect of Paris saponin I on radiosensitivity in a gefitinib-resistant lung adenocarcinoma cell line. Oncol Lett 2014; 7: 2059–2064
4 *Huang C, Xu D, Xia Q, Wang P, Rong C, Su Y.* Reversal of p-glycoprotein-mediated multidrug resistance of human hepatic cancer cells by astragaloside II. J Pharm Pharmacol 2012; 64: 1741–1750
5 *Park HJ, Kwon SH, Lee JH, Lee KH, Miyamoto K, Lee KT.* Kalopanaxsaponin A is a basic saponin structure for the anti-tumor activity of hederagenin monodesmosides. Planta Med 2001; 67: 118–121
6 *Choi JH, Lee HW, Park HJ, Kim SH, Lee KT.* Kalopanaxsaponin A induces apoptosis in human leukemia U937 cells through extracellular Ca^{2+} influx and caspase-8 dependent pathways. Food Chem Toxicol 2008; 46: 3486–3492
7 *Swamy SM, Huat BT.* Intracellular glutathione depletion and reactive oxygen species generation are important in alpha-hederin-induced apoptosis of P388 cells. Mol Cell Biochem 2003; 245: 127–139
8 *Lorent J, Le Duff CS, Quetin-Leclercq J, Mingeot-Leclercq MP.* Induction of highly curved structures in relation to membrane permeabilization and budding by the triterpenoid saponins, alpha- and delta-hederin. J Biol Chem 2013; 288: 14000–14017
9 *Shany S, Bernheimer AW, Grushoff PS, Kim KS.* Evidence for membrane cholesterol as the common binding site for cereolysin, streptolysin O and saponin. Mol Cell Biochem 1974; 3: 179–186
10 *Gelsomino G, Corsetto PA, Campia I, Montorfano G, Kopecka J, Castella B, Gazzano E, Ghigo D, Rizzo AM, Riganti C.* Omega 3 fatty acids chemosensitize multidrug resistant colon cancer cells by down-regulating cholesterol synthesis and altering detergent resistant membranes composition. Mol Cancer 2013; 12: 137
11 *Jiang YS, Jin ZX, Umehara H, Ota T.* Cholesterol-dependent induction of dendrite formation by ginsenoside Rh2 in cultured melanoma cells. Int J Mol Med 2010; 26: 787–793
12 *Ishida H, Hirota Y, Nakazawa H.* Effect of sub-skinning concentrations of saponin on intracellular Ca^{2+} and plasma membrane fluidity in cultured cardiac cells. Biochim Biophys Acta 1993; 1145: 58–62
13 *Kwon HY, Kim EH, Kim SW, Kim SN, Park JD, Rhee DK.* Selective toxicity of ginsenoside Rg3 on multidrug resistant cells by membrane fluidity modulation. Arch Pharm Res 2008; 31: 171–177
14 *Billheimer JT, Chamoun D, Esfahani M.* Defective 3-ketosteroid reductase activity in a human monocyte-like cell line. J Lipid Res 1987; 28: 704–709
15 *Kritharides L, Christian A, Stoudt G, Morel D, Rothblat GH.* Cholesterol metabolism and efflux in human THP-1 macrophages. Arterioscler Thromb Vasc Biol 1998; 18: 1589–1599
16 *De Pace DM, Esfahani M.* The effects of cholesterol depletion on cellular morphology. Anat Rec 1987; 219: 135–143
17 *Wang Y, Chen Z, Liao Y, Mei C, Peng H, Wang M, Guo H, Lu H.* Angiotensin II increases the cholesterol content of foam cells via down-regulating the expression of ATP-binding cassette transporter A1. Biochem Biophys Res Commun 2007; 353: 650–654
18 *Martelli AM, Zweyer M, Ochs RL, Tazzari PL, Tabellini G, Narducci P, Bortul R.* Nuclear apoptotic changes: an overview. J Cell Biochem 2001; 82: 634–646
19 *Lorent J, Lins L, Domenech O, Quetin-Leclercq J, Brasseur R, Mingeot-Leclercq MP.* Domain formation and permeabilization induced by the saponin alpha-hederin and its aglycone hederagenin in a cholesterol-containing bilayer. Langmuir 2014; 30: 4556–4569
20 *King MA, Radicchi-Mastroianni MA.* Effects of caspase inhibition on camptothecin-induced apoptosis of HL-60 cells. Cytometry 2002; 49: 28–35
21 *Parasassi T, Gratton E, Yu WM, Wilson P, Levi M.* Two-photon fluorescence microscopy of laurdan generalized polarization domains in model and natural membranes. Biophys J 1997; 72: 2413–2429
22 *Sanchez SA, Gunther G, Tricerri MA, Gratton E.* Methyl-beta-cyclodextrins preferentially remove cholesterol from the liquid disordered phase in giant unilamellar vesicles. J Membr Biol 2011; 241: 1–10
23 *Gauthier C, Legault J, Girard-Lalancette K, Mshvildadze V, Pichette A.* Haemolytic activity, cytotoxicity and membrane cell permeabilization of semi-synthetic and natural lupane- and oleanane-type saponins. Bioorg Med Chem 2009; 17: 2002–2008
24 *Bangham AD, Horne RW, Glauert AM, Dingle JT, Lucy JA.* Action of saponin on biological cell membranes. Nature 1962; 196: 952–955
25 *Kay JG, Murray RZ, Pagan JK, Stow JL.* Cytokine secretion via cholesterol-rich lipid raft-associated SNAREs at the phagocytic cup. J Biol Chem 2006; 281: 11949–11954
26 *Petrovic N, Schacke W, Gahagan JR, O'Conor CA, Winnicka B, Conway RE, Mina-Osorio P, Shapiro LH.* CD13/APN regulates endothelial invasion and filopodia formation. Blood 2007; 110: 142–150
27 *Kroemer G, Galluzzi L, Vandenabeele P, Abrams J, Alnemri ES, Baehrecke EH, Blagosklonny MV, El Deiry WS, Golstein P, Green DR, Hengartner M, Knight RA, Kumar S, Lipton SA, Malorni W, Nunez G, Peter ME, Tschopp J, Yuan J, Piacentini M, Zhivotovsky B, Melino G.* Classification of cell death: recommendations of the nomenclature committee on cell death 2009. Cell Death Differ 2009; 16: 3–11
28 *Anderson TM, Clay MC, Cioffi AG, Diaz KA, Hisao GS, Tuttle MD, Nieuwkoop AJ, Comellas G, Maryum N, Wang S, Uno BE, Wildeman EL, Gonen T, Rienstra CM, Burke MD.* Amphotericin forms an extramembranous and fungicidal sterol sponge. Nat Chem Biol 2014; 10: 400–406
29 *Xu ZX, Ding T, Haridas V, Connolly F, Gutterman JU.* Avicin D, a plant triterpenoid, induces cell apoptosis by recruitment of Fas and downstream signaling molecules into lipid rafts. PLoS One 2009; 4: e8532
30 *Yi JS, Choo HJ, Cho BR, Kim HM, Kim YN, Ham YM, Ko YG.* Ginsenoside Rh2 induces ligand-independent Fas activation via lipid raft disruption. Biochem Biophys Res Commun 2009; 385: 154–159
31 *Garcia-Saez AJ, Buschhorn SB, Keller H, Anderluh G, Simons K, Schwille P.* Oligomerization and pore formation by equinatoxin II inhibit endocytosis and lead to plasma membrane reorganization. J Biol Chem 2011; 286: 37768–37777
32 *Montero J, Morales A, Llacuna L, Lluis JM, Terrones O, Basanez G, Antonsson B, Prieto J, Garcia-Ruiz C, Colell A, Fernandez-Checa JC.* Mitochondrial cholesterol contributes to chemotherapy resistance in hepatocellular carcinoma. Cancer Res 2008; 68: 5246–5256
33 *Li YC, Park MJ, Ye SK, Kim CW, Kim YN.* Elevated levels of cholesterol-rich lipid rafts in cancer cells are correlated with apoptosis sensitivity induced by cholesterol-depleting agents. Am J Pathol 2006; 168: 1107–1118
34 *Chwalek M, Lalun N, Bobichon H, Ple K, Voutquenne-Nazabadioko L.* Structure-activity relationships of some hederagenin diglycosides: haemolysis, cytotoxicity and apoptosis induction. Biochim Biophys Acta 2006; 1760: 1418–1427
35 *Juin P, Pelletier M, Oliver L, Tremblais K, Gregoire M, Meflah K, Vallette FM.* Induction of a caspase-3-like activity by calcium in normal cytosolic extracts triggers nuclear apoptosis in a cell-free system. J Biol Chem 1998; 273: 17559–17564
36 *Gamble W, Vaughan M, Kruth HS, Avigan J.* Procedure for determination of free and total cholesterol in micro- or nanogram amounts suitable for studies with cultured cells. J Lipid Res 1978; 19: 1068–1070
37 *Bartlett GR.* Phosphorus assay in column chromatography. J Biol Chem 1959; 234: 466–468
38 *Tennant JR.* Evaluation of the trypan blue technique for determintion of cell viability. Transplantation 1964; 2: 685–694
39 *Servais H, Van Der Smissen P, Thirion G, Van der Essen G, Van Bambeke F, Tulkens PM, Mingeot-Leclercq MP.* Gentamicin-induced apoptosis in LLC-PK1 cells: involvement of lysosomes and mitochondria. Toxicol Appl Pharmacol 2005; 206: 321–333
40 *Hathaway WE, Newby LA, Githens JH.* The acridine orange viability test applied to bone marrow cells. I. Correlation with trypan blue exclusion and eosin dye exclusion and tissue culture transformation. Blood 1964; 23: 517–525
41 *Owen DM, Rentero C, Magenau A, Abu-Siniyeh A, Gaus K.* Quantitative imaging of membrane lipid order in cells and organisms. Nat Protoc 2012; 7: 24–35

Electronic reprint for personal use

Supporting Information

α-Hederin Induces Apoptosis, Membrane Permeabilization and Morphologic Changes in Two Cancer Cell Lines Through a Cholesterol-Dependent Mechanism

Joseph H. Lorent[1, 2], Catherine Léonard[1], Marthe Abouzi[1], Farida Akabi[1], Joëlle Quetin-Leclercq[2], Marie-Paule Mingeot-Leclercq[1]

Affiliations

[1]Université Catholique de Louvain, Louvain Drug Research Institute, Cellular and Molecular Pharmacology, Bruxelles, Belgium

[2]Université catholique de Louvain, Louvain Drug Research Institute, Pharmacognosy, Bruxelles, Belgium

Correspondence

Prof. Dr. Marie-Paule Mingeot-Leclercq

UCL B1.73.05

Avenue E. Mounier 73

B-1200 Bruxelles

Belgium

Phone : +3227647374

marie-paule.mingeot@uclouvain.be

© Georg Thieme Verlag KG · 10.1055/s-0042-114780 · Planta Med · Lorent JH et al.

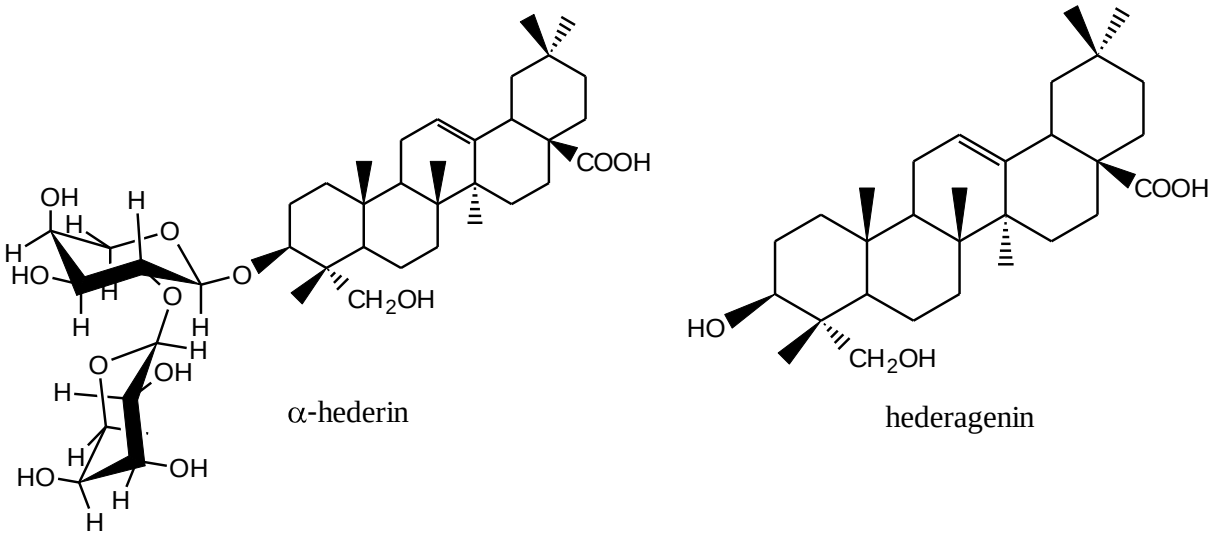

Fig. 1S Molecular structures of α-hederin and its aglycone hederagenin.

© Georg Thieme Verlag KG · 10.1055/s-0042-114780 · Planta Med · Lorent JH et al.

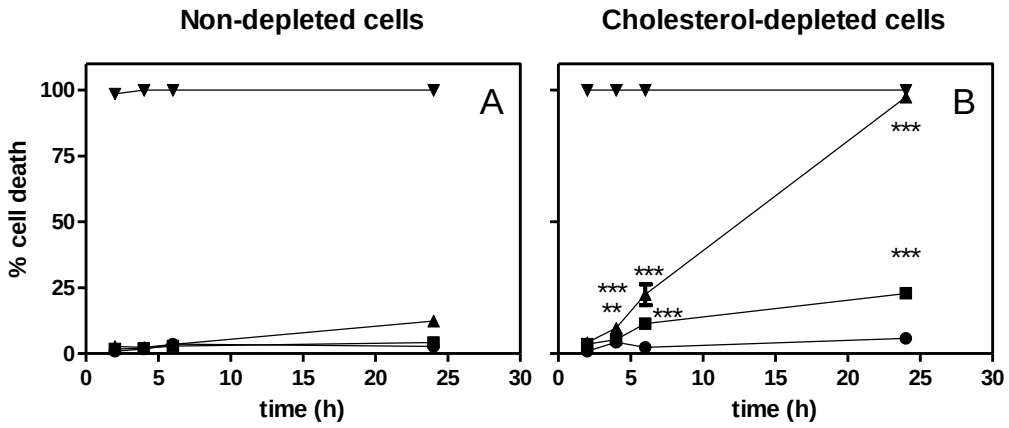

Fig. 2S Trypan blue assay in non-depleted (**A**) and cholesterol-depleted U937 cells (**B**) of increasing concentrations of sodium dodecyl sulfate (SDS): Control (●), 100 µM (■), 250 µM (▲) and 500 µM (▼). Statistical analysis: Two-way ANOVA between non-depleted and cholesterol depleted conditions. **P < 0.1, ***p < 0.01.

© Georg Thieme Verlag KG · 10.1055/s-0042-114780 · Planta Med · Lorent JH et al.

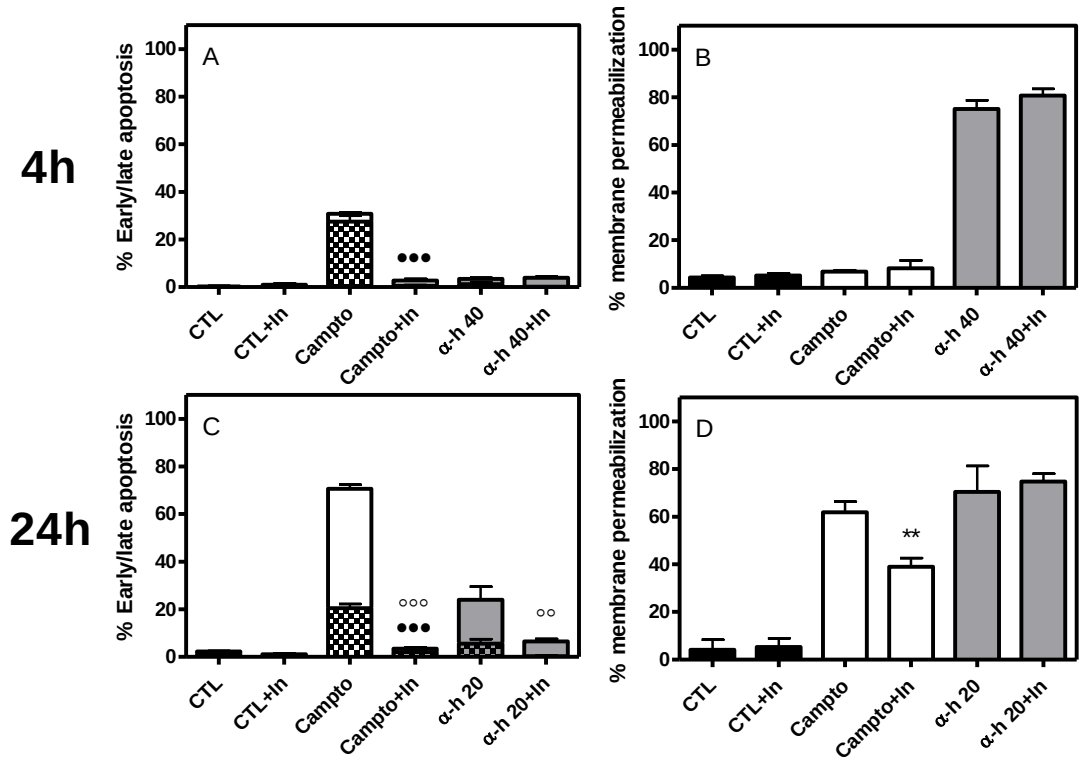

Fig. 3S Acridine orange/ethidium bromide assay of U937 cells. Early/late apoptosis (**A**, **C**) and membrane permeabilization (**B**, **D**) for cells incubated with or without general caspases inhibitor Q-VD-OPh. Camptothecine (Campto, white) has been used as a positive control for apoptosis induction. α-Hederin (α-h, grey) has been used at 20 µM and 40 µM for 24h and 4h of incubation, respectively. Statistical analysis for conditions with or without inhibitor: One way ANOVA. Symbols: ● = early apoptosis, ○ =late apoptosis, * =membrane permeabilization; two symbols : $p < 0.01$, three symbols: $p < 0.001$.

© Georg Thieme Verlag KG · 10.1055/s-0042-114780 · Planta Med · Lorent JH et al.

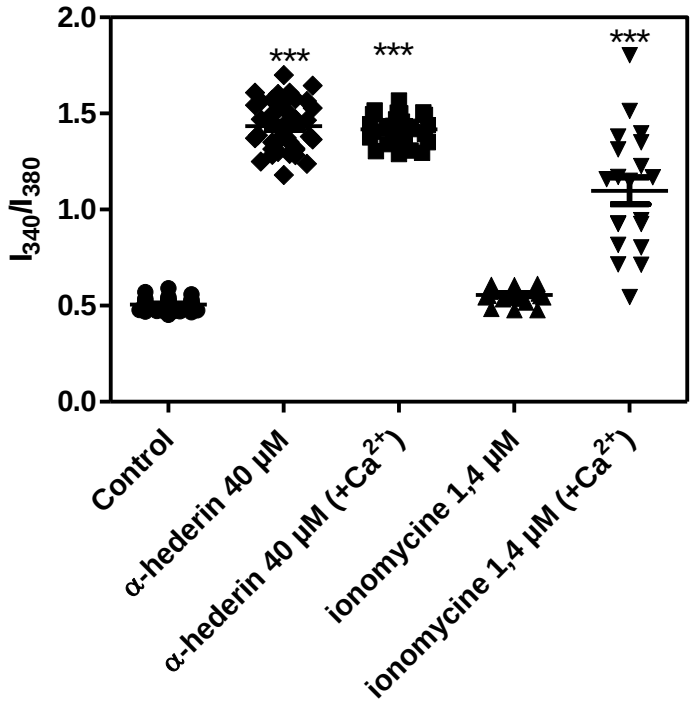

Fig. 4S Intensity ratio of Ca^{2+} bound vs. unbound FURA-2 in U937 cells after 5 min of incubation with α-hederin in media containing Ca^{2+} ions (+Ca^{2+}) or not. Statistical analysis: One way ANOVA was used to compare intensity ratios to the control. ***P < 0.001.

© Georg Thieme Verlag KG · 10.1055/s-0042-114780 · Planta Med · Lorent JH et al.

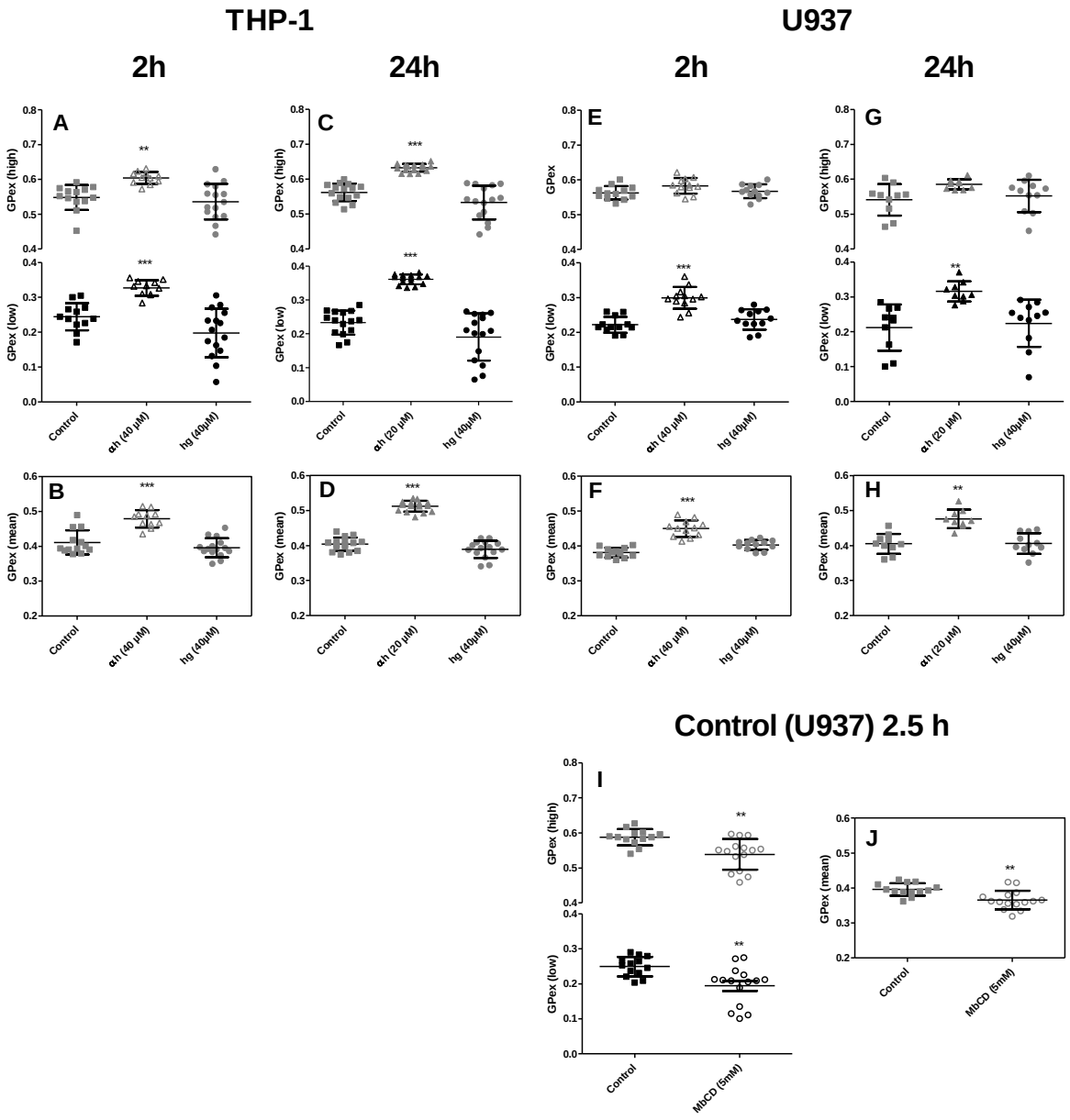

Fig. 5S GP-data of THP-1 (**A**, **B**, **C**, **D**) and U937 (**E**, **F**, **G**, **H**) cells. Panel **A**, **C**, **E**, **G**, **I**: GP-values of a GP image have been fitted to a double Gaussian function centered at GPex (low), black colors and GPex (high), grey colors. Panel **B**, **D**, **F**, **H**, **J**: Average of all GP-values in a GP-image. Statistical analysis, two-way ANOVA compared to control. **P < 0.01, ***p < 0.001.

© Georg Thieme Verlag KG · 10.1055/s-0042-114780 · Planta Med · Lorent JH et al.